Addressing Cultural Heritage Challenges: Applications of Open-Access Remote Sensing Datasets for Monitoring Threats

Kyriakos Michaelides[1*], Stylianos Hadjipetrou[1], Athos Agapiou[1], Apostolos Sarris[2], Victor Klinkenberg[2], Miltiadis Polidorou[2]

[1] Dept. of Civil Engineering and Geomatics, Faculty of Engineering and Technology, Cyprus University of Technology, Saripolou 2 8, 3036 Limassol, Cyprus – [*]km.michaelides@edu.cut.ac.cy, s.hadjipetrou@cut.ac.cy, athos.agapiou@cut.ac.cy
[2] Digital Humanities GeoInformatics Lab, Sylvia Ioannou Chair on Digital Humanities, Archaeological Research Unit, Department of History and Archaeology, University of Cyprus, Gladstone 12, 1095 Nicosia, Cyprus – sarris.apostolos@ucy.ac.cy, klinkenberg.victor@ucy.ac.cy, polidorou.miltiadis@ucy.ac.cy

Keywords: Remote sensing, heritage preservation, soil erosion, RUSLE, GIS.

Abstract

This study investigates soil erosion risks in various European heritage sites using open-access satellite remote sensing data and the Revised Universal Soil Loss Equation (RUSLE) methodology. The aim is to assess and visualize erosion risks to support the sustainable management and preservation of cultural heritage sites. Results show significant soil loss in several areas, with many exceeding the tolerable threshold of 1 t/ha/yr, indicating the need for targeted conservation strategies. In Monti Lucretili, over 61% of the area experiences moderate to extreme soil loss, while Sant'Antonio di Ranverso, Baltanás, and Delos Island also face considerable erosion threats. Sant'Antonio and Delos show 12.66% and 14.76% of their areas at high to very high risk, respectively. In Baltanás, 66% experiences low to moderate erosion, around 31% is at high to very high risk, and only 2.27% faces severe erosion. A unified methodology was applied across all study areas, integrating multi-temporal satellite data to estimate erosion risks. This approach combines RUSLE and GIS to produce a model that identifies areas requiring immediate attention. Results were validated against RUSLE 2010 and 2015 datasets provided by ESDAC, showing consistent patterns, with minor differences due to spatial resolution and terrain characteristics. Through spatial analysis techniques such as trend analysis and multi-temporal integration, this study offers valuable insights for land management. The findings highlight the critical role of remote sensing tools in assessing and mitigating soil erosion risks, which is essential for safeguarding cultural heritage under ongoing environmental and anthropogenic pressures.

1. Introduction

Soil erosion threatens cultural heritage sites, particularly in regions with steep terrain and fragile land cover (Borrelli et al., 2017; Panagos et al., 2015). It weakens site stability, accelerates land degradation, and affects biodiversity and ecosystems (FAO, 2019). Understanding soil loss is crucial for conservation efforts in European heritage sites, where erosion poses significant risks (Blanco & Lal, 2008).

The Revised Universal Soil Loss Equation (RUSLE) is widely used to assess erosion rates under various conditions (Renard et al., 1997). Integrating RUSLE with GIS and remote sensing enables spatial analysis, supporting large-scale erosion assessments (Mitasova et al., 1996). In remote heritage locations lacking ground-based monitoring, open-access satellite imagery offers an effective alternative for tracking erosion trends (Lu et al., 2004).

This study applies RUSLE, combined with the use of GIS and remote sensing to evaluate soil erosion risks in European heritage sites. The research identifies high-risk areas where soil loss surpasses sustainable levels, guiding conservation efforts (Panagos et al., 2020). Multi-temporal satellite data help visualize erosion patterns, assisting decision-makers in protecting cultural sites (Ganasri & Ramesh, 2016).

A consistent methodology was used across study locations, including Baltanás (Spain), Sant'Antonio di Ranverso and Monti Lucretili (Italy), and Delos Island (Greece). The analysis indicates significant erosion in some areas, with parts exceeding the tolerable limit of 1 t/ha/yr, underscoring the need for sustainable land management (Poesen et al., 2003). The spatial distribution of erosion highlights the role of topography, vegetation, and soil properties in erosion vulnerability (Wischmeier & Smith, 1978).

This study provides a framework for assessing erosion risks in heritage landscapes using geospatial techniques. This approach highlights the value of geospatial analysis in conservation, supporting proactive strategies to mitigate erosion and protect cultural heritage from environmental and human-induced threats.

2. Materials and Methods

This study applied a unified methodology across all study areas to assess and visualize erosion risks. This approach used open-access satellite remote sensing products, as these areas lack ground-based monitoring. The methodology is based on the RUSLE in combination with GIS. This process developed an erosion risk assessment model using visual programming techniques (Figure 1).

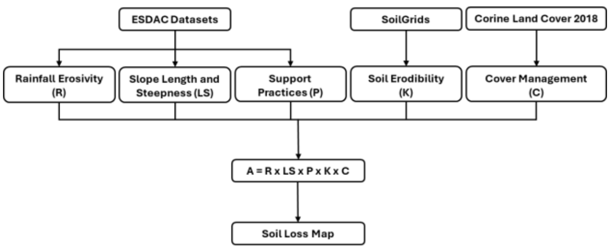

Figure 1. Risk assessment model flow chart

2.1 Study Area

This study examines four distinct European sites (Figure 2) with unique historical, cultural, and environmental features. Despite their differences, all are relatively remote from major urban centers, preserving their character.

The Cellar Town of Baltanás (41.93898 N, -4.24439 W) in Spain, 40 km from Palencia, hosts the country's largest underground cellar complex—374 cellars carved into clay soil, ensuring stable conditions for traditional winemaking. The area spans 221.86 km², with elevations from 724 to 916 meters.

The Sant'Antonio di Ranverso Preceptory (42.08983 N, 12.87230 E) in Italy, 20 km west of Turin, is a religious complex founded in 1188. It played a key role in medieval pilgrimage and healthcare. Covering nearly 400 km², it features Gothic architecture at elevations between 244 and 1,608 meters.

The Monti Lucretili (42.08983 N, 12.87230 E) northeast of Tivoli, Rome, forms the core of a regional natural park. Spanning 1,528.7 km², with peaks up to 1,505 meters, it contains rich forests and archaeological remains, including the Roman Villa of Horace and UNESCO-listed dry-stone walls.

The Island of Delos (37.39333 N, 25.27111 E) in the Aegean Sea near Mykonos is a key archaeological site and the mythical birthplace of Apollo and Artemis. Covering just 80.95 km², it was inscribed on the UNESCO World Heritage List in 1990.

Despite their geographic diversity, these sites offer valuable insights into heritage conservation, environmental conditions, and European historical site management.

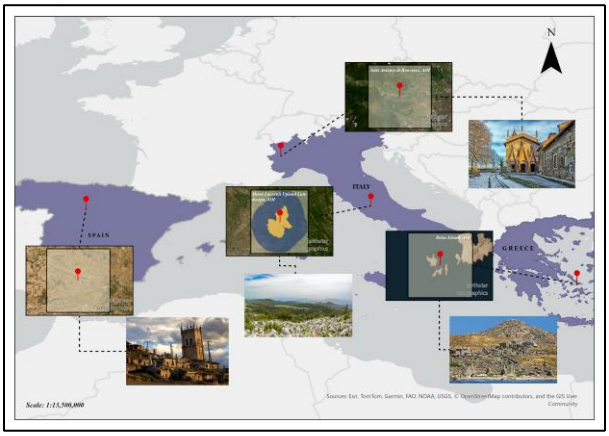

Figure 2. Study area locations

2.2 Soil Erosion Estimation

Soil erosion was estimated by integrating open-access satellite remote sensing products (See Table 1) with the RUSLE model within a GIS environment (ArcGIS Pro 3.4.1).

Data Type	Spatial Resolution	Source
Rainfall Erosivity (R)	-	*GloREDa - ESDAC (https://esdac.jrc.ec.europa.eu/content/global-rainfall-erosivity* ,accessed on 15 January 2025)
Soil Erodibility (K)	250m x 250m	SoilGrids - global gridded soil information ISRIC (https://www.isric.org/explore/soilgrids ,accessed on 15 January 2025)
Cover Management (C)	-	CORINE Land Cover 2018 – LMS Copernicus (https://land.copernicus.eu/en/products/corine-land-cover/clc2018 ,accessed 15 January 2025)
Slope Length and Steepness (LS)	25m x 25m	Slope Length and Steepness factor (LS-factor) – ESDAC (https://esdac.jrc.ec.europa.eu/themes/slope-length-and-steepness-factor-ls-factor ,accessed on 15 January 2025)
Support Practices (P)	-	Mean P-factor (NUTS2) – ESDAC (https://esdac.jrc.ec.europa.eu/content/support-practices-factor-p-factor-eu ,accessed on 15 January 2025)

Table 1. Spatial resolution of data and source

Each RUSLE factor was derived from standardized EU datasets, ensuring data consistency and accuracy. The factors were either generated using available geospatial data or extracted from authoritative European datasets, including long-term rainfall records, high-resolution soil property maps, and detailed land use classifications. These datasets provided reliable inputs for modeling soil erosion within the GIS environment. The methodological workflow followed is presented in Figure 1.

Individual factor layers and thematic maps were generated and processed within the ArcGIS environment using a standardized cell grid, achieving a spatial resolution of 5 meters to ensure spatial consistency. Furthermore, the coordinate reference system for each study area was defined using the corresponding Universal Transverse Mercator (UTM) zone, ensuring geospatial accuracy.

The average annual soil erosion rate was then calculated by applying Equation 1, combining the factor layers within the RUSLE model. The results were visualized through classified maps, following the classification standards established by the Joint Research Centre (JRC).

The RUSLE model is a multiplicative function of five factors that control water erosion. The soil loss is calculated by the following equation (Wischmeier & smith, 1978; Renard et al., 1991):

$$A = R \times K \times C \times LS \times P \tag{1}$$

where A represents the annual average soil loss (t ha^{-1} year^{-1}), R is the rainfall erosivity factor (MJ mm ha^{-1} h^{-1} year^{-1}), K is the soil erodibility factor (t ha h ha^{-1} MJ^{-1} mm^{-1}), C is the cover-management factor (dimensionless), LS is the slope length and slope steepness factor (dimensionless) and P is the support practices factor (dimensionless).

2.2.1 Rainfall Erosivity factor (R factor)

Rainfall erosivity factor quantifies the impact of rainfall on soil detachment and transport, depending on rainfall intensity and total precipitation. Higher-intensity storms produce greater erosive energy, increasing the risk of soil erosion. In this study, R-factor values were obtained from the European Soil Data Centre (ESDAC) Global Rainfall Erosivity Database (GloREDa) (See Table 1), which provides standardized erosivity data derived from high-resolution precipitation records across multiple meteorological stations. The dataset includes long-term average R-values, calculated based on sub-hourly rainfall intensity measurements and kinetic energy estimations.

To generate a continuous spatial representation of rainfall erosivity, the Inverse Distance Weighting (IDW) interpolation method was applied in ArcGIS. This technique estimates R-values for unsampled locations by weighting nearby station values based on their distance, ensuring a smooth transition of erosivity across the study area. The interpolated R-factor raster was then used as an input in the RUSLE model to assess soil erosion potential.

2.2.2 Soil Erodibility factor (K factor)

The soil erodibility factor represents the susceptibility of soil to erosion based on its physical and chemical properties. It is influenced by soil texture, organic matter content, structure, and permeability, which determine how easily soil particles can be detached and transported by rainfall and runoff.

The soil property data were obtained from SoilGrids (See Table 1), a global gridded soil information system developed by ISRIC. Specifically, the dataset includes values for sand, silt, clay, and soil organic matter content, which were used to calculate the K factor. The estimation follows the empirical equation proposed by Wischmeier and Smith (1978):

$$K=2.8\times10^{-7}\times(12-OM)\times M^{1.14}+4.3\times10^{-3}\times(s-2)+3.3\times10^{-3}\times(p-3) \quad (2)$$

Where K is the soil erodibility factor (t ha h ha^{-1} MJ^{-1} mm^{-1}), is the soil structure class (s=1: very fine granular, s=2: fine granular, s=3, medium or coarse granular, s=4: blocky, platy or massive), p is the permeability class (p=1: very rapid, …, p=6: very slow). OM is the percent of organic matter content and can be estimated (Van Bemmelen, 1890; Pribyl, 2010):

$$OM = \%SOC \times 1.724 \quad (3)$$

M is the textural factor and is calculated as

$$M = (\%silt + (\%sand \times 0.1)) \times (100 - \%clay) \quad (4)$$

2.2.3 Cover management factor (C factor)

The Cover management factor represents the effect of vegetation and land cover on soil erosion. It quantifies how different types of land cover influence soil loss reduction by intercepting rainfall, reducing runoff velocity, and stabilizing the soil surface. Lower C-values indicate better protection against erosion, while higher values represent surfaces more susceptible to soil loss (Panagos et al., 2015).

This study used the Corine Land Cover (CLC) 2018 dataset (See Table 1) to determine the C-Factor values. The procedure involved obtaining the CLC 2018 vector layer and identifying reference values for different land cover types. Each CLC code was then assigned a corresponding C factor based on values found in the literature. An Excel table containing these values was created and subsequently joined to the attribute table of the CLC 2018 dataset in GIS software. The final step involved converting the vector dataset into raster format, using the C factor values as the attribute field, to generate a continuous spatial representation suitable for use in the RUSLE model.

2.2.4 Topographic factor (LS factor)

The Topographic factor is an important component in soil erosion modeling, representing the combined effects of slope length (L) and slope steepness (S) on soil erosion potential. It quantifies how the land's topography, particularly its slope, influences water runoff and soil detachment, with steeper and longer slopes leading to higher erosion rates.

This study obtained the LS factor data from the ESDAC LS Factor Map (See Table 1), which provides global data at a 25m resolution for each country. The data were processed by setting the appropriate coordinate system and adjusting the spatial resolution to meet the specific needs of the study. Following this, the dataset was clipped to the Area of Interest (AOI) for each region, ensuring that only the relevant areas were included in the analysis, thereby improving the accuracy of the soil erosion estimates.

2.2.5 Supporting practice factor (P factor)

The supporting practice factor represents the effect of conservation practices, such as contouring, terracing, or strip cropping, on reducing soil erosion. This factor accounts for how different land management practices influence the amount of soil loss, with higher P-values indicating less effective conservation measures and lower P-values reflecting more effective soil conservation practices.

For this study, data on the P factor were obtained from the ESDAC Mean P-factor dataset (See Table 1), which provides regional (NUTS2) level values for the European Union. The mean P-factor values for each case study area were extracted and used to calculate the corresponding P factor for each region. In the next step, a constant raster was created in a GIS environment, where the spatial resolution and coordinate system were set appropriately. Finally, the raster was clipped to the AOI for each region, ensuring the analysis was focused on the relevant study areas.

3. Results & Discussion

Once the raster layers for each factor (R, K, C, LS, and P) were generated in a GIS environment, the next step was to estimate the annual soil loss for each study area. This was achieved by applying the RUSLE model, integrating the individual factors to calculate the potential soil erosion values for the respective regions.

GIS provides essential spatial and analytical functions, enabling efficient geo-referencing, spatial overlays, and data processing across different scales. The study classified the soil erosion results into eight categories (See Table 2) based on erosion risk, as defined by the JRC, allowing for a detailed visualization of spatial variability in soil erosion and supporting a more comprehensive understanding of erosion risks across the study areas.

Erosion Category	Numeric Range (t/ha/year)	Severity Index
1	0 – 0.5	Negligible
2	0.5 – 1	Very Low
3	1 – 2	Low
4	2 – 5	Moderate
5	5 – 10	High
6	10 – 20	Very High
7	20 – 50	Severe
8	>50	Extreme

Table 2. Soil Erosion Severity Classification

3.1 R factor

Rainfall erosivity analysis across the study areas indicates a strong correlation between altitude and rainfall intensity. The R factor map highlights regions with significant elevation, such as Monti Lucretili, Sant'Antonio di Ranverso, and Baltanás, which experience higher rainfall erosivity values, increasing erosion susceptibility. In contrast, Delos Island, with its lower elevation, exhibits relatively lower R values, suggesting a reduced erosion impact of rainfall. The spatial distribution of rainfall erosivity reveals that adjacent high-altitude areas also experience elevated R values (See Table 3), further intensifying erosion risks. These findings emphasize the role of topography in influencing rainfall erosivity patterns and are critical for evaluating R factor values. The R factor maps are shown in Figure 3.

Study Area	**R Factor (MJ mm ha⁻¹ h⁻¹ year⁻¹)**		
	Min	**Max**	**Mean**
Baltanás, Spain	1241.15	1338.11	1312.22
Sant'Antonio di Ranverso, Italy	1776.36	2324.93	1915.74
Monti Lucretili, Italy	1609.74	2604.77	1930.11
Delos Island, Greece	1192.01	1252.22	1230.95

Table 3. R Factor Values

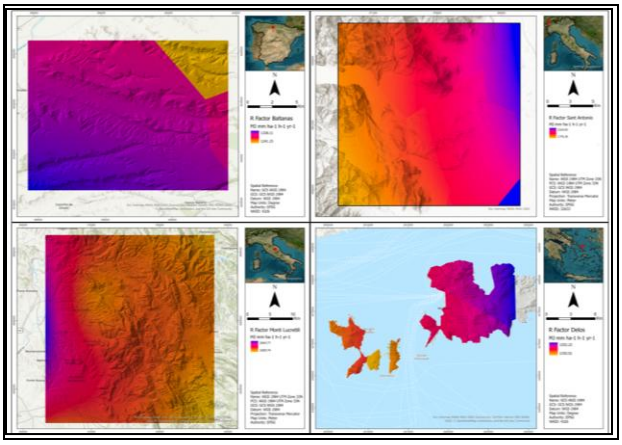

Figure 3. R factor maps

3.2 K factor

The mean K factor values (See Table 4) across the study areas indicate variations in soil erodibility, reflecting the soil's susceptibility to erosion due to its physical and chemical properties. The highest mean K factor is observed in Baltanás, suggesting a moderate level of soil erodibility. Delos Island follows, indicating slightly lower but still notable erodibility. In contrast, Sant'Antonio di Ranverso and Monti Lucretili exhibit relatively lower erodibility. The K factor maps are shown in Figure 4.

Study Area	**K Factor (t ha h ha⁻¹ MJ⁻¹ mm⁻¹)**		
	Min	**Max**	**Mean**
Baltanás, Spain	0.004	0.030	0.021
Sant'Antonio di Ranverso, Italy	0	0.050	0.013
Monti Lucretili, Italy	-0.006	0.039	0.010
Delos Island, Greece	0.004	0.030	0.018

Table 4. K factor values

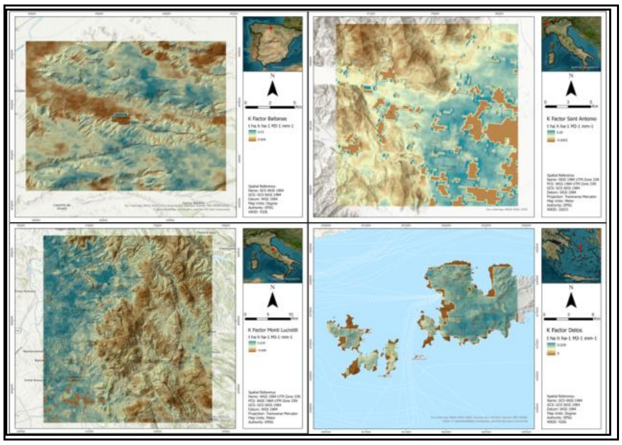

Figure 4. K factor maps

3.3 C factor

The C factor values (See Table 5), representing the cover management effect on soil erosion, vary across the study areas, reflecting differences in land cover and vegetation. Baltanás exhibits the highest mean C factor, indicating greater susceptibility to erosion due to lower vegetation cover or more erosion-prone land use practices. In contrast, Sant'Antonio di Ranverso has the lowest mean C factor, suggesting better protective vegetation cover or land management practices that reduce erosion risk. Monti Lucretili and Delos show moderate values, indicating varying levels of vegetation cover and land use impact. The maximum C factor values recorded in Monti Lucretili and Baltanás highlight areas within these regions that are particularly prone to erosion due to sparse vegetation or intensive land use. These results emphasize the role of land cover management in mitigating soil erosion risks across different landscapes. The C factor maps are shown in Figure 5.

Study Area	**C Factor**		
	Min	**Max**	**Mean**
Baltanás, Spain	0	0.30	0.21
Sant'Antonio di Ranverso, Italy	0	0.25	0.08
Monti Lucretili, Italy	0	0.40	0.13
Delos Island, Greece	0	0.30	0.11

Table 5. C factor values

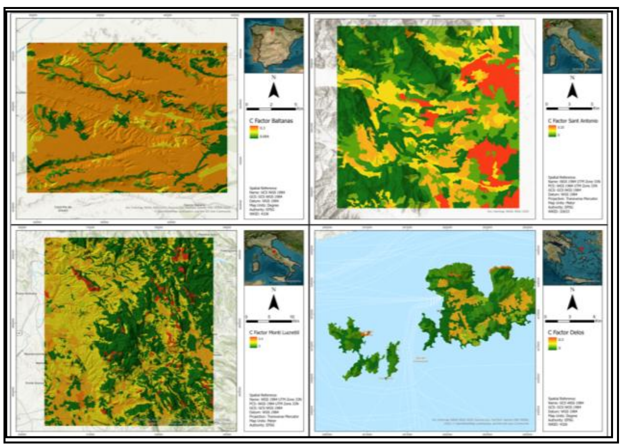

Figure 5. C factor maps

3.4 LS factor

The LS factor values (See Table 6), representing the combined effects of slope length and steepness on soil erosion, were extracted from the ESDAC dataset, which provides global data at a 25m resolution. The results for the study areas are shown in Figure 6. Since the LS factor is derived from topography, steeper slopes and higher elevation variations correspond to higher LS values, increasing erosion susceptibility. Monti Lucretili has the highest mean LS factor, followed by Sant'Antonio di Ranverso and Delos, indicating significant topographic variation. In contrast, Baltanás exhibits the lowest mean LS factor, suggesting flatter terrain with lower erosion potential. Maximum LS values reach 91.40 in Sant'Antonio di Ranverso and 90.39 in Monti Lucretili, particularly along riverbanks and rugged landscapes. However, in Baltanás and other relatively low-relief study areas, the topographic factors are lower, reducing the influence of slope on erosion.

Study Area	Ls factor		
	Min	Max	Mean
Baltanás, Spain	0.03	17.75	1.08
Sant'Antonio di Ranverso, Italy	0.03	91.40	2.93
Monti Lucretili, Italy	0.03	90.39	3.88
Delos Island, Greece	0.03	66.17	2.45

Table 6. LS factor values

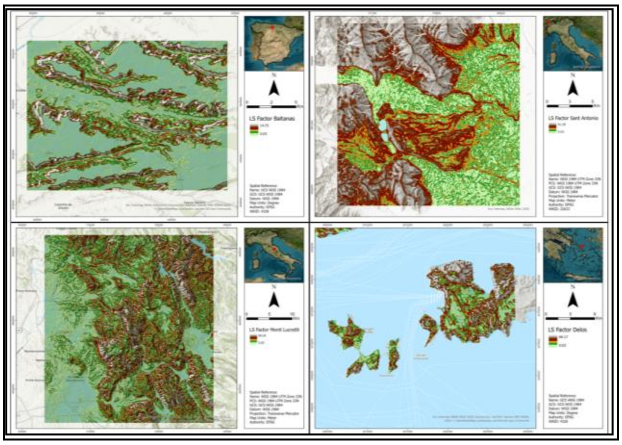

Figure 6. LS factor maps

3.5 P factor

The P factor represents the influence of soil conservation practices on surface runoff and erosion reduction. The values range from 0 to 1, where higher values indicate minimal or no erosion control measures. In this study, the mean P factor values for the selected areas (See Table 7) reveal that Monti Lucretili and Sant'Antonio di Ranverso exhibit the highest values, suggesting limited or nearly non-existent erosion control measures. Baltanás follows with slightly lower values, still indicating minimal conservation efforts. In contrast, Delos Island has the lowest P factor among the study areas, reflecting relatively better conservation practices. The P factor maps are shown in Figure 7.

Study Area	P factor
	Mean
Baltanás, Spain	0.93
Sant'Antonio di Ranverso, Italy	0.95
Monti Lucretili, Italy	0.98
Delos Island, Greece	0.76

Table 7. P factor values

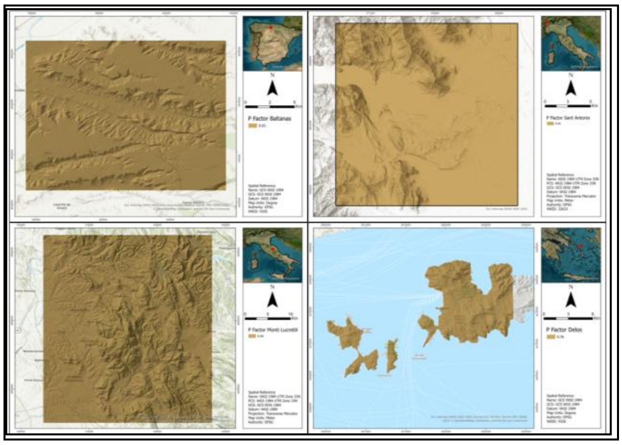

Figure 7. P factor maps

3.6 Soil Loss

Soil erosion is a critical environmental issue that threatens land productivity and ecosystem stability. The RUSLE, combined with GIS and remote sensing techniques, provides an effective method for quantifying soil loss and assessing erosion risk across different landscapes. This study evaluates soil loss across four distinct regions: Baltanás, Sant'Antonio di Ranverso, Monti Lucretili, and Delos Island. These areas represent diverse geomorphological and climatic conditions, influencing soil erosion's severity and spatial distribution.

The results indicate that soil loss varies significantly between the study sites, ranging from negligible to extreme erosion. While low erosion rates predominantly characterize some regions, others exhibit significant areas under high to severe erosion, necessitating urgent conservation measures. The spatial patterns of soil loss, as visualized in GIS-based maps, highlight the necessity for region-specific soil management strategies to mitigate degradation and promote sustainable land use.

The spatial distribution of soil loss in Baltanás, presented in Figure 8, highlights areas of higher vulnerability, particularly in regions with steep slopes, low vegetation cover, and high soil erodibility.

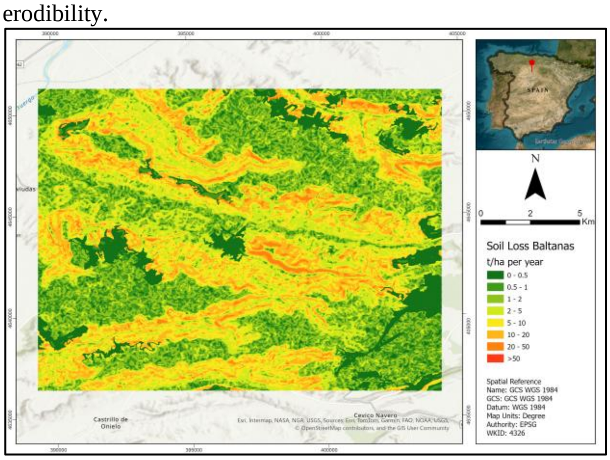

Figure 8. Baltanás soil erosion map

The analysis highlights varying degrees of soil erosion in the study area (See Table 8). Negligible and very low soil loss account for around 23%, indicating minimal risk. Most of the land (43%) falls under low to moderate erosion, reflecting a notable impact. High and very high erosion zones cover about 31%, signaling increased vulnerability. Severe and extreme erosion, though limited to 2.66%, represent critical areas needing targeted conservation.

Study Area	Class	Severity Index	Soil Loss (t/ha/yr)	Area (ha)	Area (%)
Baltanás, Spain	1	Negligible	0 – 0.5	2100.24	9.46
	2	Very Low	0.5 – 1	2950.04	13.30
	3	Low	1 – 2	5054.86	22.78
	4	Moderate	2 – 5	4642.72	20.93
	5	High	5 – 10	4013.92	18.10
	6	Very High	10 – 20	2919.13	13.16
	7	Severe	20 – 50	505.37	2.27
	8	Extreme	>50	0.39	0
	Total			22186.67	100

Table 8. Soil Erosion Risk Distribution in Baltanás

The estimated soil loss in Sant'Antonio di Ranverso ranges from negligible to extreme. The spatial distribution of soil erosion, illustrated in Figure 9, highlights vulnerable areas, particularly those with steep slopes, sparse vegetation, and highly erodible soils.

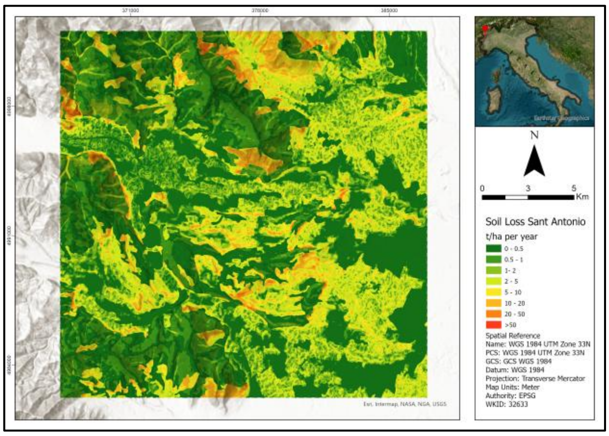

Figure 9. Sant'Antonio di Ranverso soil erosion map

The analysis shows that a large portion of the area experiences minimal erosion, with over half classified as negligible to very low. Low to moderate erosion affects a notable share of the landscape, while high and very high erosion zones, covering more than 12%, are concentrated in steeper terrains. Although severe and extreme erosion are limited, they indicate critical areas requiring focused conservation efforts (See Table 9).

Study Area	Class	Severity Index	Soil Loss (t/ha/yr)	Area (ha)	Area (%)
Sant'Antonio di Ranverso, Italy	1	Negligible	0 – 0.5	14201.99	35.51
	2	Very Low	0.5 – 1	8677.31	21.69
	3	Low	1 – 2	5260.23	13.15
	4	Moderate	2 – 5	6663.29	16.66
	5	High	5 – 10	3191.39	7.98
	6	Very High	10 – 20	1708.99	4.27
	7	Severe	20 – 50	289.07	0.72
	8	Extreme	>50	7.50	0.02
	Total			39999.71	100

Table 9. Soil Erosion Risk Distribution in Sant'Antonio di Ranverso

The assessment of soil loss in Monti Lucretili reveals a wide range of erosion severity. The spatial distribution of erosion, as depicted in Figure 10, highlights areas most at risk, particularly those with steep slopes, sparse vegetation, and highly erodible soils.

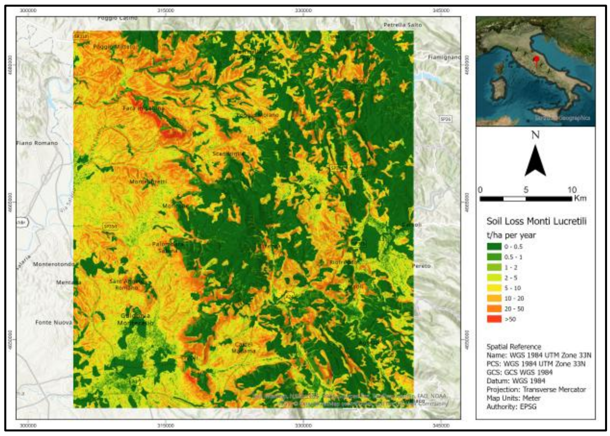

Figure 10. Monti Lucretili soil erosion map

The findings show that 35.43% of the study area experiences negligible soil loss, while 6.84% falls under the very low category. Low soil loss is observed in 3.55%, and 10.26% experience moderate erosion. High and very high erosion zones account for 15.10% and 19.25%, respectively. Severe erosion affects 9.05% of the area, while extreme soil loss is minimal at 0.52% (See Table 10).

Study Area	Class	Severity Index	Soil Loss (t/ha/yr)	Area (ha)	Area (%)
Monti Lucretili, Italy	1	Negligible	0 – 0.5	54157.65	35.43
	2	Very Low	0.5 – 1	10467.99	6.84
	3	Low	1 – 2	5432.59	3.55
	4	Moderate	2 – 5	15679.17	10.26
	5	High	5 – 10	23087.56	15.10
	6	Very High	10 – 20	29422.13	19.25
	7	Severe	20 – 50	13835.81	9.05
	8	Extreme	>50	789.17	0.52
	Total			152872.1	100

Table 10. Soil Erosion Risk Distribution in Monti Lucretili

The soil loss assessment for Delos Island indicates varying degrees of erosion severity. The spatial distribution of soil loss, illustrated in Figure 11, highlights areas of higher vulnerability, particularly in regions with limited vegetation cover, steep terrain, and susceptible soil types.

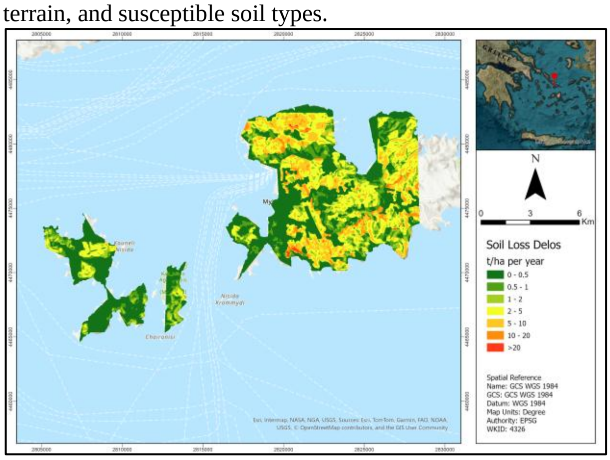

Figure 11. Delos Island soil erosion map

The analysis indicates that a significant portion of Delos Island experiences minimal soil loss, with a substantial area falling under negligible to low erosion. Moderate erosion affects a notable share of the land, highlighting areas where soil degradation is more pronounced. Meanwhile, high and very high erosion zones, though less extensive, still present concerns for land stability. Severe erosion is limited to a small fraction of the study area, representing isolated zones of intense soil loss (See Table 11).

Study Area	Class	Severity Index	Soil Loss (t/ha/yr)	Area (ha)	Area (%)
Delos Island, Greece	1	Negligible	0 – 0.5	3064.21	37.85
	2	Very Low	0.5 – 1	965.94	11.93
	3	Low	1 – 2	918.33	11.35
	4	Moderate	2 – 5	1929.05	23.83
	5	High	5 – 10	976.25	12.06
	6	Very High	10 – 20	218.3	2.70
	7	Severe	>20	22.58	0.28
	Total			8094.66	100

Table 11. Soil Erosion Risk Distribution in Delos Island

The results highlight significant soil erosion risks across the study areas, with large portions exceeding the tolerable threshold of 1 t/ha/yr, emphasizing the need for targeted conservation strategies. Integrating multi-temporal remote sensing datasets enables improved spatial analysis of erosion patterns, offering a more comprehensive understanding of soil degradation over time. Since the RUSLE model primarily estimates sheet and rill erosion (Renard et al., 1997), these insights contribute to informed land management decisions and enhance the long-term preservation of vulnerable landscapes.

To ensure the reliability of the estimated soil loss rasters for the four study areas, these results were validated against RUSLE 2010 and RUSLE 2015 datasets provided by the ESDAC at a 100m resolution. Statistical metrics, including mean and standard deviation, were used for comparison and are presented in Figure 12. The validation revealed that the mean and standard deviation values from the estimated soil loss rasters at 5m resolution were consistent with the 100m resolution RUSLE 2010 and RUSLE 2015 datasets, with minor differences mainly attributed to the difference in spatial resolution. This confirms the accuracy of the estimated soil loss data, ensuring their reliability for further analysis and applications in soil erosion risk management.

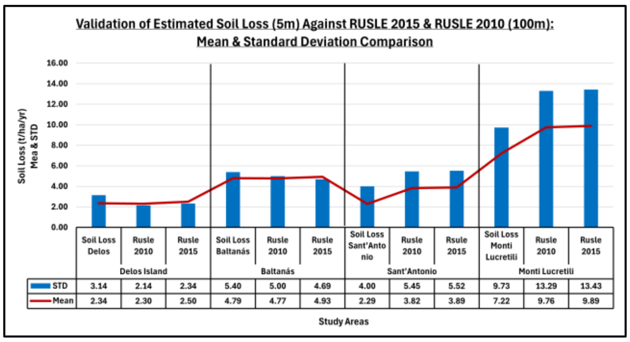

Figure 12. Comparison of Estimated Soil Loss with ESDAC RUSLE Datasets Across Study Areas

In Delos Island and Baltanás, the 5m resolution data showed slightly higher soil loss values, reflecting better detection of localized topographic and land cover variation. Sant'Antonio showed minimal differences, indicating strong agreement between the two datasets. However, in Monti Lucretili, the 5m estimates were noticeably lower than those from the 100m dataset. This discrepancy may be due to the area's large size and complex terrain, which can introduce smoothing effects and variations in how erosion patterns are represented across scales. The lower values may indicate a tendency of the higher-resolution model to slightly underrepresent broad erosion patterns. Nevertheless, despite this potential underestimation, soil erosion in Monti Lucretili remains a significant issue, as indicated by the high proportion of the area falling into moderate to extreme erosion classes.

This validation demonstrates that the estimated soil loss data are reliable and suitable for further analysis and soil erosion risk management applications.

4. Conclusion

This study emphasizes the integration of remote sensing, GIS and the RUSLE to assess soil erosion risks across European cultural heritage sites. The findings reveal significant spatial variability in erosion, with several study areas exceeding the tolerable soil loss threshold of 1 t/ha/yr. Monti Lucretili, Italy, exhibited over 61% of its area experiencing moderate to extreme soil loss, while Sant'Antonio di Ranverso, Italy, and Delos Island, Greece, also showed high erosion risks, with 12.66% and 14.76% of their areas at high to very high risk, respectively. In Baltanás, Spain, 66% of the area experiences low to moderate erosion, around 31% is at high to very high risk, and only 2.27% faces severe erosion.

To ensure the reliability of these estimates, the results were validated against the RUSLE 2010 and 2015 datasets from ESDAC. The validation showed that the 5m resolution soil loss rasters are largely consistent with the 100m reference datasets. Minor discrepancies were observed such as slightly higher values in Baltanás and Delos, reflecting enhanced detail captured by finer spatial resolution, and lower values in Monti Lucretili, likely due to the area's complex terrain and large extent, which may have led to a slight underestimation. Nevertheless, the validation supports the overall accuracy and applicability of the approach for erosion risk assessment.

Using multi-temporal satellite data and geospatial analysis, this research provides a reliable methodology for assessing erosion risk across diverse landscapes. Key factors such as topography, rainfall erosivity, vegetation cover, and land management practices influenced soil loss patterns, with the R, K, C, LS, and P factors highlighting the complex interactions between natural and anthropogenic forces.

This approach offers a cost-effective way to monitor erosion in heritage sites, especially where field data is limited. The study's findings underscore the need for proactive mitigation measures, such as vegetation restoration, erosion control, and sustainable land-use planning, to protect cultural landscapes from environmental degradation.

Future research will expand the analysis by incorporating factors such as urban expasnion, floods, fire risk, and displacements through a multi-criteria analysis approach. Enhancing predictive models and integrating additional datasets will improve erosion forecasts and support the long-term preservation of cultural heritage sites.

Acknowledgments

Funded by the European Union. Views and opinions expressed are however those of the author(s) only and do not necessarily reflect those of the European Union or REA. Neither the European Union nor the granting authority can be held responsible for them (ARGUS PROJECT - Grant Agreement Number 101132308).

References

Blanco, H., Lal, R. (2008). Principles of Soil Conservation and Management. Springer, Dordrecht. doi.org/10.1007/978-1-4020-8709-7.

Borrelli, P., Robinson, D.A., Fleischer, L.R., Lugato, E., Ballabio, C., Alewell, C., Meusburger, K., Modugno, S., Schütt, B., Ferro, V., Bagarello, V., van Oost, K., Montanarella, L., Panagos, P. (2017). An assessment of the global impact of 21st-century land use change on soil erosion. Nature Communications, 8, 2013. doi.org/10.1038/s41467-017-02142-7.

Borrelli, P., Robinson, D.A., Fleischer, L.R., Panagos, P. (2020). An assessment of soil erosion prevention strategies in European policies. Land Use Policy, 90, 104305.

FAO (2019). Soil erosion: the greatest challenge for sustainable soil management. Food and Agriculture Organization of the United Nations, Rome. www.fao.org/3/ca4396en/ca4396en.pdf.

Ganasri, B.P., Ramesh, H. (2016). Assessment of soil erosion by RUSLE model using remote sensing and GIS – A case study of Nethravathi Basin. Geoscience Frontiers, 7(6), 953-961. doi.org/10.1016/j.gsf.2015.10.007.

Lu, D., Li, G., Valladares, G.S., Batistella, M. (2004). Mapping soil erosion risk in Rondonia, Brazilian Amazonia using RUSLE, remote sensing, and GIS. Land Degradation & Development, 15(5), 499-512. doi.org/10.1002/ldr.634.

Mitasova, H., Hofierka, J., Zlocha, M., Iverson, L.R. (1996). Modelling topographic potential for erosion and deposition using GIS. International Journal of Geographical Information Systems, 10(5), 629-641. doi.org/10.1080/02693799608902101.

Panagos, P., Borrelli, P., Meusburger, K. (2015). A new European soil erosion model based on land cover and rainfall data. Environmental Science & Policy, 54, 438-447. doi.org/10.1016/j.envsci.2015.07.017.

Panagos, P., Borrelli, P., Meusburger, K., Alewell, C., Lugato, E., Montanarella, L. (2015). Estimating the soil erosion cover-management factor at the European scale. Land Use Policy, 48, 38-50.

Panagos, P., Borrelli, P., Poesen, J., Ballabio, C., Lugato, E., Meusburger, K., Montanarella, L., Alewell, C. (2020). The new assessment of soil loss by water erosion in Europe. Environmental Research, 187, 109678. doi.org/10.1016/j.envres.2020.109678.

Poesen, J., Nachtergaele, J., Verstraeten, G., Valentin, C. (2003). Gully erosion and environmental change: importance and research needs. Catena, 50(2-4), 91-133. doi.org/10.1016/S0341-8162(02)00143-1.

Pribyl, D.W. (2010). A critical review of the conventional SOC to SOM conversion factor. Geoderma, 156(3-4), 75-83.

Renard, K.G., Foster, G.R., Weesies, G.A., McCool, D.K., Yoder, D.C. (1991). Predicting soil erosion by water: A guide to conservation planning with the Revised Universal Soil Loss Equation (RUSLE). U.S. Department of Agriculture.

Renard, K.G., Foster, G.R., Weesies, G.A., McCool, D.K., Yoder, D.C. (1997). Predicting soil erosion by water: A guide to conservation planning with the Revised Universal Soil Loss Equation (RUSLE). U.S. Department of Agriculture, Agricultural Research Service.

Van Bemmelen, J.M. (1890). Die chemische Zusammensetzung der Ackerkrume. Landwirtschaftliche Versuchsstationen, 37, 279-290.

Wischmeier, W.H., Smith, D.D. (1978). Predicting Rainfall Erosion Losses – A Guide to Conservation Planning. U.S. Department of Agriculture, Agricultural Handbook 537.